A New Comprehensive Framework for Cascading Outage Simulation in Power Systems

Moossa Khodadadi Arpanahi
Luxembourg Institute of Science and Technology (LIST)
Belvaux, Luxembourg
moossa.khodadadi@list.lu

Florin Capitanescu
Luxembourg Institute of Science and Technology (LIST)
Belvaux, Luxembourg
florin.capitanescu@list.lu

***Abstract*— Simulating accurately and fast cascading outages play a critical role in power system security and resilience assessment. This paper proposes a new comprehensive framework for cascading outage simulation, articulated around an extended AC power flow. To address the key modelling features of cascading outage simulation, the proposed framework develops new algorithms for: a) detecting possible islanding, b) frequency control in each island: primary frequency control (PFC), under-frequency load shedding (UFLS) and over-frequency generator tripping (OFGT) and c) improved under-voltage load shedding (UVLS) and load models to avoid the divergence of AC power flow and allow handling voltage instability during the cascade. Tests on a realistic 60-bus system show that the proposed cascading outage simulator can successfully handle islanding, PFC, UFLS, OFGT, and UVLS; it simulates the cascade until there is no violation of system frequency, voltage, and power flow limits in islands that do not experience blackout.**

***Index Terms*-- AC power flow, cascading outage simulation, frequency control, islanding, voltage instability.**

I. Introduction

Cascading outages are triggered by an initial asset outage and consist in a sequence of disconnections of power system assets. They can significantly impair the power system's main function of meeting demand and lead to a widespread system blackout (e.g., Italy in 2003, parts of USA and Canada in 2003). Due to the massive and costly consequences of cascading outages, accurate analysis, risk assessment, and management are required [1]-[2]. Simulating precisely yet fast cascading outages is a growing need due to climate change and thereby grid resilience concerns.

In this context, several simulation models for cascading outages have been developed, which, as shown in Table I, can be classified according to several key modelling features such as: a) handling the possible system islanding, b) modelling frequency control to maintain power balance in each island by automatic primary frequency control (PFC) as well as under-frequency load shedding (UFLS) and over-frequency generator tripping (OFGT) protection schemes, and c) modelling voltage protection scheme e.g. under-voltage load shedding (UVLS). However, these features have been rarely and partly investigated in the literature. For instance, islanding detection, a prerequisite for the simulation of cascading outages, has been explored [3]-[4] but it received limited attention within the cascading outage scope.

There are two general modelling approaches to cascading outage simulation: (i) steady-state, based on DC power flow (DC PF) [5]-[8] or AC power flow (AC PF) [9]-[20], and (ii) dynamic simulation [21]-[24]. Each approach trades-off differently precision and computation time. Although dynamic simulation provides the best insight into what happens during cascading outages, it suffers from large computation time, e.g. if an initiating event triggers multiple cascades and islands (in other words the simulated time and new strong dynamics may occur as opposite to the simulation of a short-circuit followed by dynamics being damped out after tens of seconds), and many initiating events have to be considered in real time. To avoid, on the one hand, the oversimplifications of the DC PF and, on the other hand, the heavy computations of the dynamic simulation, most existing cascading outage simulators rely on the AC PF model, which is a reasonable compromise accuracy vs speed.

A common issue during cascading outages is the active power imbalance in the islands created, which may severely affect the island frequency. In practice, such frequency deviation is compensated by frequency controllers (PFC and, if required, UFLS/OFGT). However, the conventional AC PF, which is commonly used in cascading outage simulation [9]-[20], cannot capture accurately the PFC, UFLS and OFGT models as the power flow does not explicitly model the system frequency.

Another important aspect of AC PF-based cascading outage simulation models that has not been adequately addressed is the modelling of UVLS, a control scheme designed to protect the system against voltage instability. Ignoring or inaccurately modelling the UVLS results in an unrealistic simulation of power system behaviour during a cascading outage. Indeed, DC PF-based methods neglect the UVLS because they are not designed to capture voltage issues. On the other hand, the AC PF-based methods face the issue of power flow divergence during simulation e.g., when the system is close or beyond its loadability limit and hence prone to voltage instability. To circumvent this issue, the existing approaches either consider this situation as the blackout of the corresponding island due to a voltage collapse and stop the simulation for the island or use some over-simplified assumptions to achieve a converged AC PF solution and pursue the simulation. However, both approaches lead to an unrealistic model of the system behaviour for severe

TABLE I. TAXONOMY OF CASCADING OUTAGE SIMULATORS BASED ON DIFFERENT KEY MODELLING FEATURES.

Reference	Simulation Type	Feature				
		Islanding	PFC	UFLS/ OFGT	UVLS	VDL
[5], [6]	DC-PF			○		
[8]-[11]	AC/DC-PF			○	◍	
[12]	AC-PF			●	◍	
[6]	DC-PF			●	◍	
[13], [14]	AC-PF			●	◍	
[15]-[17]	PF/TDS		○	○	○	○
[18]	AC-PF			◍	◍	
[19]	AC-PF		●	●	◍	●
[7]	DC-PF		●	●		
[20]	TDS			○	●	
[21]	TDS			○	●	
[22]	TDS		●	●	●	●
Proposed	AC-PF	●	●	●	●	●

Blank field means the feature is not considered; ○: Considered but details are not mentioned; ◍: Simply considered; ●: Considered. PF: Power Flow; OPF: Optimal Power Flow; TDS: Time-Domain Simulation; UFLS: Under-Frequency Load Shedding; PFC: Primary Frequency Control; UVLS: Under-Voltage Load Shedding; OFGT: Over-Frequency Generator Tripping; VDL: Voltage Dependent Loads.

voltage issues, that impacts the outcome of the subsequent cascade simulation.

The more accurate modelling of the various aspects, inadequately addressed, of cascading outage simulation, detailed so far, motivates us to revisit and enhance existing cascading outage simulation models. This paper proposes a new and comprehensive AC-PF-based framework for cascading outage simulation, with the following specific novel contributions:

- ✓ The islands created following each single or multiple contingencies are accurately identified using a new algorithm called linear dependency-based islanding detection (LIBID).
- ✓ A new algorithm is proposed to handle the active power balance within each island considering all possible frequency controllers (PFC, UFLS and OFGT) as well as power limits of the generators.
- ✓ A new enhanced UVLS model to tackle voltage instability. In the proposed model, once the system is prone to voltage instability, leading to AC PF divergence and hindering cascading outage simulation to proceed, an extended AC PF is applied to approximate the final operating point of the system. This model makes possible the operation of UVLS and mimics the behaviour of the system while avoiding power flow divergence.
- ✓ An extended AC PF is proposed, which is at the core of the simulator, whose two extensions are: (i) generators participation to PFC, which extends AC PF with distributed slack generators [25] to calculate the frequency, and (ii) voltage dependent loads (VDL).

The rest of the paper is organized as follows. Section II presents the proposed AC-SS-based framework for simulating cascading outage. Section III presents the results of the study on the Nordic 60-bus system and illustrates in detail the ability of the proposed framework to address various aspects of the cascade problem. Finally, Section IV concludes.

II. OUTLINE OF THE PROPOSED CASCADING OUTAGE SIMULATION FRAMEWORK

A general overview of the proposed framework for simulating cascading outages is shown in Fig. 1. The goal is to simulate the behaviour of the system when an initiating event triggers a

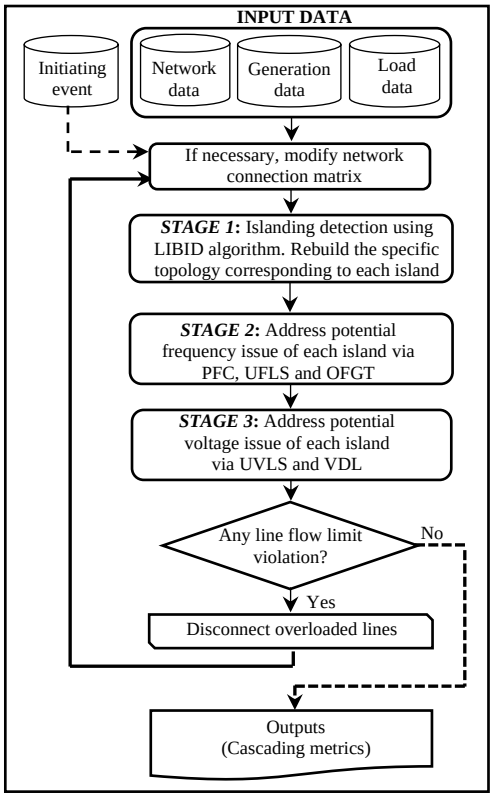

Figure 1. Generic outline of the proposed framework for cascading outage simulation.

sequence of outages. The proposed method models the action of the existing emergency frequency and voltage control systems during the cascade, so that the results obtained are as close as possible to reality.

As illustrated in Fig. 1, a special input is an initiating event (e.g., a single or multiple contingencies such as line or generator trip). In addition, network, generation, and load data are provided as additional inputs. If necessary (e.g., after a line disconnection), the network connection matrix must be modified.

The proposed framework comprises three main stages, denoted as *STAGE 1* to *3*, presented in detail hereafter.

STAGE 1 checks if the system splits into islands and identifies the resulted islands using the LIBID algorithm. Note that in this stage, as one of the main aspects of the implementation, the specific topology of each island is rebuilt. This means renumbering the equipment and determining which generators, loads, lines, and transformers are present in each island and cascade (i.e., an iteration of the algorithm shown in Fig. 1).

STAGE 2 deals with potential frequency issues (both under-frequency and over-frequency) in each island. In practice, there are automatic control actions to deal with frequency problems both normal control (PFC) and emergency control (UFLS and OFGT). The potential frequency issues are identified and addressed by implementing these three automatic controllers. To increase accuracy, an extended (frequency-embedded) AC PF is proposed that takes into account the participation of all generators in the active power balance and also considers network effects (i.e., power loss, voltages, and reactive powers). Some of these

aspects are usually neglected in AC PF-based cascading outage simulators.

STAGE 3 identifies voltage issues and tackles them through a realistic model of the UVLS protection. Simulating voltage issues during cascading outages based on AC PF is one of the challenges of AC PF-based models because after *STAGE 2*, it may happen that the voltage of some buses drop very low or AC PF diverges, which prevents continuing the simulation. However, as it will be explained in subsection II-D, the proposed algorithm can be used to simulate existing UVLS schemes based on AC power flow overcoming the issue of power flow divergence.

According to Fig. 1, after performing *STAGES 1* to *3* for all islands, the line flow limits are checked, and if any is violated, the corresponding lines are disconnected. The disconnection of such lines, as new contingencies, leads to a new operating state of the system and, in general, to some new islands. The algorithm proceeds iteratively until there is no violation of the frequency, voltage, and line flow limits (frequency and voltage violations are already addressed in *STAGES 2* and *3*, respectively).

The simulation output are the following metrics:

$$LO = \sum_{c,l} {b_l}^c \qquad LNS = \sum_{c,l} |\Delta {P_{Li}}^c| \qquad GT = \sum_{c,i} |\Delta {P_{Gi}}^c| \tag{1}$$

where LO, LNS, and GT denote the number of line outages, the amount of load not supplied, and the amount of generation tripped, respectively. The indices i and c refer to buses of the system and cascades (i.e., an iteration of the algorithm shown in Fig. 1). The binary variable ${b_l}^c$ indicates whether the line l is failed or not during the c^{th} cascade. Also, $\Delta {P_{Li}}^c$ and $\Delta {P_{Gi}}^c$ are the amount of load shedding and generation tripping at bus i in cascade c.

In the following, first, the extended AC PF in *STAGES 2* and *3* is presented. Then, *STAGES 1* to *3* are explained in detail.

A. Extended AC Power Flow Considering PFC and VDL

AC PF-based cascading outage simulation models rely on the conventional power flow formulation, wherein the active power of all generators, except the slack, is held constant. The physical meaning of such modeling is that only one generator ($\mathbb{B}^{S0}$) responds to an active power imbalance within the system. However, in practice, following a contingency, multiple generators ($\mathbb{B}^{S}$) engage in maintaining active power balance. They collectively work to keep the system frequency within acceptable limits using the so-called PFC mechanism or the droop control functionality of governors. As a result, assuming the active power of such generators remains fixed is inaccurate, as it is a function of system frequency, denoted as f.

Furthermore, the conventional AC PF assumes a load model of constant active and reactive powers (PQ-constant). However, active and reactive powers are voltage dependent.

To enhance the precision of cascading outage simulation, an extended AC PF is integrated into *STAGES 2* and *3* of the proposed simulator. This enhanced AC PF, detailed below, considers both PFC and VDL, ensuring a more accurate representation of system behaviour during cascading outages.

To calculate the post-contingency operating point of the system considering the PFC effect of generation units, system frequency, and voltage dependency of loads, AC power flow equations are extended as follows.

$$\forall i \in \mathbb{B} \tag{2}$$
$$\Delta P_i(\boldsymbol{V}, \boldsymbol{\delta}, \Delta f) = (P_{Gi}^0 - d_{Gi}\Delta f) - P_{Li}^0(d_p {V_i}^{\alpha}) - \sum_{j\in\mathbb{B}} V_i V_j\left(g_{ij}\cos(\delta_i - \delta_j) + b_{ij}\sin(\delta_i - \delta_j)\right)$$

$$\forall i \in \mathbb{B}^{PQ}: \tag{3}$$
$$\Delta Q_i(\boldsymbol{V}, \boldsymbol{\delta}, \Delta f) = -Q_{Li}^0\left(d_q {V_i}^{\alpha}\right) - \sum_{j\in\mathbb{B}} V_i V_j\left(g_{ij}\sin(\delta_i - \delta_j) - b_{ij}\cos(\delta_i - \delta_j)\right)$$

where V, δ, P, and Q refer to voltage magnitude, voltage angle, active power, and reactive power, respectively. In addition, the subscripts G and L refer to generator and load, and superscript "0" denotes the initial (pre-contingency) value of the variable. Also, $\mathbb{B}$ and $\mathbb{B}^{PQ}$ represent the set of all buses and PQ buses of the network, and i and j are indices of the buses. Real and imaginary parts of $(i,j)^{th}$ element of admittance matrix $\boldsymbol{Y}$ are represented by g_{ij} and b_{ij}, respectively. The parameter d_{Gi} denotes generator governor droop while load demand characteristics are described by the parameters d_p, d_q, and α. The frequency deviation Δf is defined as

$$\Delta f = f - f^0 \tag{4}$$

Note that, as (2) shows, the extended AC power flow has an additional active power balance equation corresponding to the slack bus of conventional AC power flow, $\mathbb{B}^{S0}$. Therefore, active power balance equation is applied to all buses $\mathbb{B}$. It should be noted that, considering system frequency as a new variable, still the number of unknown state variables and equations are the same. The presence of frequency as a new variable and dependency of the active and reactive power of the load on the voltage are also reflected in the Jacobian matrix (5), in which the vectors $\boldsymbol{\mathcal{P}}$, $\boldsymbol{\delta}$, $\boldsymbol{\mathcal{Q}}$, and $\boldsymbol{V}$ are defined as (6).

$$\boldsymbol{\mathcal{J}}^E = \begin{bmatrix} \frac{\partial \boldsymbol{\mathcal{P}}}{\partial \boldsymbol{\delta}} & \frac{\partial \boldsymbol{\mathcal{P}}}{\partial \boldsymbol{V}} & \frac{\partial \boldsymbol{\mathcal{P}}}{\partial \Delta f} \\ \frac{\partial \boldsymbol{\mathcal{Q}}}{\partial \boldsymbol{\delta}} & \frac{\partial \boldsymbol{\mathcal{Q}}}{\partial \boldsymbol{V}} & \frac{\partial \boldsymbol{\mathcal{Q}}}{\partial \Delta f} \end{bmatrix} \tag{5}$$

$$\boldsymbol{\mathcal{P}} = \{P_i |\, i \in \mathbb{B}\},\ \boldsymbol{\delta} = \{\delta_i |\, i \in \mathbb{B} - \mathbb{B}^{S0}\} \tag{6a}$$

$$\boldsymbol{\mathcal{Q}} = \{Q_i |\, i \in \mathbb{B}^{PQ}\},\ \boldsymbol{V} = \{V_i |\, i \in \mathbb{B}^{PQ}\} \tag{6b}$$

The expressions for $\partial\boldsymbol{\mathcal{P}}/\partial\boldsymbol{\delta}$, $\partial\boldsymbol{\mathcal{Q}}/\partial\boldsymbol{\delta}$, $\partial\boldsymbol{\mathcal{P}}/\partial\boldsymbol{V}$, and $\partial\boldsymbol{\mathcal{Q}}/\partial\boldsymbol{V}$ are the same in the conventional and extended models, except for an additional term, stemming from VDL, in each element of $\partial\boldsymbol{\mathcal{P}}/\partial\boldsymbol{V}$ and $\partial\boldsymbol{\mathcal{Q}}/\partial\boldsymbol{V}$, which are represented as equation (7).

$$\alpha P_{Li}^0(d_p {V_i}^{\alpha-1}),\ \alpha Q_{Li}^0(d_q {V_i}^{\alpha-1}) \tag{7}$$

Also, the derivatives with respect to the frequency are as (8).

$$\frac{\partial P_i}{\partial \Delta f} = -d_{Gi} \quad , \quad \frac{\partial Q_i}{\partial \Delta f} = 0 \tag{8}$$

The procedure for solving the equations is identical to that of the conventional AC PF. During each iteration, the unknown state variable variations are calculated as follows.

$$\begin{bmatrix} \Delta \boldsymbol{\delta} \\ \Delta \boldsymbol{V} \\ \Delta f \end{bmatrix} = (\boldsymbol{\mathcal{J}}^E)^{-1} \begin{bmatrix} \Delta \boldsymbol{\mathcal{P}} \\ \Delta \boldsymbol{\mathcal{Q}} \end{bmatrix} \tag{9}$$

The extended AC power flow model offers distinct advantages over the conventional model, specifically:

1) It adopts a frequency-linked model, introducing frequency as a new variable. Consequently, it becomes possible to precisely evaluate the exact change in active power of generators due to contingencies, as illustrated in (10).

$$P_{Gi} = P_{Gi}^0 - d_{Gi}\Delta f \ , \forall \ i \in \mathbb{B}^S \tag{10}$$

2) It enables accurate assessment of potential violation in system frequency and generator active power limits, as explained in the subsection II-C.

3) The model incorporates VDL, making it versatile for use in PQ-constant mode (same as conventional AC power flow) or, if required, in Z-constant mode. The advantage of this capability will be elaborated in subsection II-D.

B. STAGE 1: Islanding Identification

Fig. 2 (a) shows the proposed LIBID algorithm developed for islanding detection. This algorithm is inspired by the concept of "row space of a matrix" [26], focusing on the use of idea of linear dependency. In summary, rows i and k of matrix $\boldsymbol{A}$ are said to be linearly independent if and only if the inner product of vectors r_i and r_i is 0, as given in equation (11).

$$r_i \odot r_k = 0 \tag{11}$$

Here, let $\boldsymbol{A} = [a_{ik}]_{n\times n}$be the connectivity matrix for the power network, where a_{ij} is defined as follows.

$$a_{ik} = \begin{cases} 1 & i = k \text{ or buses } i \text{ and } k \text{ are connected} \\ 0 & \text{buses } i \text{ and } k \text{ are not connected} \end{cases} \tag{12}$$

As shown in Fig. 2 (a), the LIBID algorithm receives an updated $\boldsymbol{A}$ matrix (it is updated after each contingency). Then, the algorithm identifies the existing islands using three nested loops.

In the innermost loop (Loop-1, with counter i), the algorithm identifies the rows of the matrix A that are linearly dependent on the first row. The corresponding row indices are then stored in the set K and subsequently removed from matrix $\boldsymbol{A}$. As Fig. 2 (a) shows, the number of all buses associated with rows specified by set K is also stored in the set $\mathcal{C}$, where $\mathcal{C}_i$ contains the elements of row i with value "1".

Loop-2, with counter j, constructs matrix $\widetilde{\boldsymbol{A}}$ that is initially null (empty), and then the j^{th} row of matrix $\widetilde{\boldsymbol{A}}$ is filled based on the members of the set $\mathcal{C}$. Indeed, each row of the matrix $\widetilde{\boldsymbol{A}}$ denotes the buses that are directly or indirectly connected. Each iteration of Loop-2 processes the remaining part of the matrix $\boldsymbol{A}$ until $\boldsymbol{A}$ becomes null. In such a case, as shown in Fig. 2 (a), $\boldsymbol{A}$ is replaced by $\widetilde{\boldsymbol{A}}$.

Loop-3, as the outer loop, iterates Loop-2 until all rows of matrix $\boldsymbol{A}$ **(**which is equal to the value of matrix $\widetilde{\boldsymbol{A}}$ at the end of Loop-2), become linearly independent. In other words, each bus is only represented in one of $\mathcal{C}_i$. Hence, the stopping criteria can be expressed as (13) where $S_{\mathcal{C}_i}$ denotes summation of all members of $\mathcal{C}_i$. Finally, every row within matrix $\boldsymbol{A}$ corresponds to one island. As mentioned in Fig. 1, this enables the reconstruction of the precise topology for each island. For instance, to obtain $\boldsymbol{Y}$ matrix linked with each island, rows and columns associated with buses of that islands are retained, while other rows and columns are excluded. Moreover, an internal renumbering is necessary for buses, generators, transformers, lines, and more in each island.

$$\sum_i S_{\mathcal{C}_i} = \frac{1}{2} n(n+1) \tag{13}$$

C. STAGE 2: Handling Frequency Issues

As shown in Fig. 2 (b), *STAGE 2* is designed to simulate system behavior following a contingency event resulting in a frequency violation within the newly formed islands (*STAGE 2* is performed for each island individually). In practice, once a contingency occurs, all generators equipped with PFC respond to it, participating to compensate the resulted active power imbalance in the system. The extended AC PF presented in subsection II-A is used to model the effect of PFC of the generating units. In addition, the resulting islands may experience a sharp drop or increase in frequency, requiring UFLS or OFGT.

As Fig. 2 (b) shows, *STAGE 2* first checks the frequency of the island. If there is an over- frequency ($\Delta f > \Delta f_{MAX}$) or under-frequency ($\Delta f < \Delta f_{MIN}$), OFGT and UFLS are performed. The OFGT and UFLS blocks will have some generation trip or load shedding to keep the frequency of each island within the allowable range. For instance, the UFLS block is performed based on a pre-specified load shedding list that includes the priority, amount, and maximum load shedding for each load. However, in both over-frequency and under-frequency, the generation change of the system is calculated based on some approximate equations, denoted by (14), since network effects such as voltages, power losses, and reactive power are not considered in these equations.

$$\Delta f = -(\textstyle\sum_i P_{Li} - \sum_i P_{Gi}) / \sum_i d_{Gi} \tag{14a}$$

$$\Delta P_{Gi} = -d_{Gi}\Delta f \quad \forall \ i \in \mathbb{B}^S \tag{14b}$$

$$P_{Gi} = P_{Gi}^0 + \Delta P_{Gi} \quad \forall \ i \in \mathbb{B}^S \tag{14c}$$

To be even more accurate and mimic the realistic behaviour of the power system during cascading outage, a more accurate simulation of the frequency adjustment of the islands can be performed. To this end, as Fig. 2 (b) shows, after performing the OFGT or UFLS block, AC power flow is calculated. However, it can be done in two different modes. The first and default mode is AC PF with constant power. However, if it does not converge, an equivalent Z-constant load model is used based on the extended AC PF presented in subsection II-A.

Noted that the switching to Z-constant load model complies with what is conventionally used in the dynamic simulation-based methods, where an exponential characteristic as in (2) and (3) is considered for loads during transient periods. For $\alpha = 2$, these models introduce a Z-constant model and can approach result of AC PF to what obtained using dynamic simulation. More

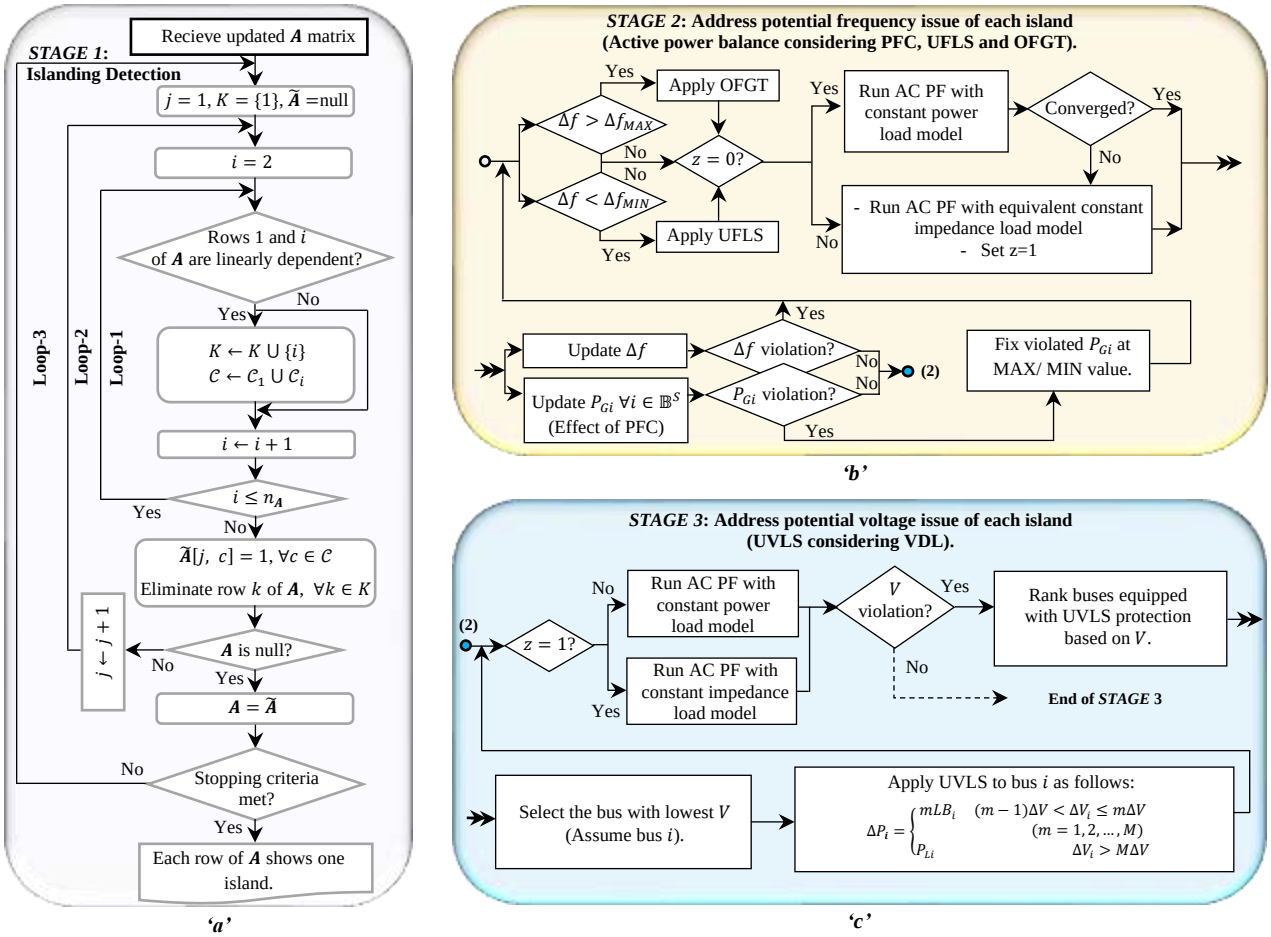

Figure 2. Detailed flowchart of the 3 stages of the proposed framework for cascading outage simulation.

importantly, this approach avoids divergence of AC PF and is especially useful for *STAGE 3* where UVLS is simulated, as will be shown in the next subsection. Note that the binary indicator z indicates AC PF mode, where $z = 0$ and $z = 1$ indicate PQ-constant and Z-constant models, respectively. In any case, after performing AC PF, the exact change of system frequency and active power generation of all slack buses is obtained.

If there is a violation of frequency or active power generation (any violated P_{Gi} is fixed at its maximum / minimum limit) *STAGE* 2 is repeated until there is no more violation of frequency or generator active power limit, and we enter *STAGE* 3.

In summary, *STAGE* 2 specifies which and how much generators and possibly loads are adjusted due to the occurrence of contingency, taking into account the network effect and the limits of system frequency and active power of generators.

D. STAGE 3: Handling Voltage Issue

As explained in the previous subsections, after each initiating or subsequent cascade, each island first maintains its frequency using PFC or UFLS/OFGT. In many cases, voltage problems occur in different buses after frequency adjustment. In such cases, the protection system responds locally to under-voltage by performing some predefined UVLS schemes. The cascading outage simulator should simulate the response of the system according to the operation of protection devices. However, due to the expectedly low voltage level, AC PF may not converge, and the system operating point may not be calculated; so it is unknown how to apply UVLS according to actual conditions.

In such cases, simulation methods for cascading failures based on AC PF use some simplifying or unrealistic assumptions that do not match real-world conditions. For example, uniform load shedding as one of the conventional methods does not correspond to reality because: (i) load shedding is started from an unknown (possibly unstable) point at which the power flow does not converge and (ii) in practice, loads are shed based on a predetermined priority list instead of shedding proportionally all loads. More importantly, the real-world UVLS protection system shed loads based on voltage values, whereas in those methods the voltage of the system is unknown and they perform load shedding without knowing the voltage values from the beginning.

As shown in Fig. 2, the proposed method takes advantage of the extended AC power flow. This is achieved by switching to a Z-constant load model in cases where the default PQ-constant model fails to converge, thereby calculating the operating point of the system. To do so, the binary indicator z is first checked to determine the convergence of the AC power flow using the PQ-constant load model (initially, z has a value of *STAGE 2*). When

$z = 1$, the extended AC power flow is executed with Z-constant load model. In any case, after the execution of the power flow, the voltage violations are checked. If any violation is detected, the algorithm selects buses equipped with UVLS protection and sheds load from the bus with the lowest voltage V as per (15).

$$\Delta P_i = \begin{cases} mLB_i & (m-1)\Delta V < \Delta V_i \le m\Delta V \\ & (m = 1, 2, \dots, M) \\ P_{Li} & \Delta V_i > M\Delta V \end{cases} \quad (15)$$

Assume that the bus i selected for UVLS includes, as in practice, M predetermined load blocks, each represented by the load demand LB_i. As the equation shows, the amount of shed load at bus i, ΔP_i, depends on the voltage drop ΔV_i. To illustrate, when $0 < \Delta V_i \le \Delta V$, a single load block is shed ($\Delta P_i = LB_i$), and for $\Delta V < \Delta V_i \le 2\Delta V$, two load blocks are shed ($\Delta P_i = 2LB_i$). When the voltage drop exceeds a predefined value ($M\Delta V$), the entire load at bus i is shed i.e. $\Delta P_i = P_{Li}$.

As Fig. 2 shows, after load shedding from bus i during *STAGE 3*, the process is repeated to check if there is still a voltage violation on the studied island. The absence of voltage violations results in the termination of *STAGE 3*. Like *STAGE 2*, *STAGE 3* is also performed for each created island.

As mentioned earlier and shown in Fig. 1, after completion of *STAGES 1* to *3*, the line violation is checked for all islands, and if there is a line violation, the next cascade is triggered. The cascading outage simulation continues until no more line violation is observed, hence no more contingency is triggered.

III. Simulation Results

The performance of the proposed cascading outage simulator is evaluated using a realistic 60-bus model of the Nordic power system, whose network connections are shown in Fig. 3. Detailed data of the system are available in [27]. We assume the allowable ranges of voltage and frequency deviation with respect to the nominal values are ±0.1 p.u. and ±0.5 Hz, respectively (these values are used for illustrative purposes and may not necessarily be realistic in every context). In addition, the following assumptions are adopted:

- The model neglects system inertia and dynamic response to frequency. The frequency after *STAGE 1* refers to the equilibrium condition.
- Similar to conventional AC power flow, generators' reactive power limits are considered by switching PV buses to PQ buses when these limits are violated.
- Load tap changers (LTC) are neglected, and there are no switchable shunt elements. Such elements are assumed to stay always connected during the cascade.

The proposed simulator was implemented using the Julia programming language on a 3.00-GHz 11th Gen Intel (R) Core (TM) i7-1185G7 CPU personal computer with 48 GB RAM. The results of two cases are presented below.

A. Case Study 1: Nordic Power System Split into Two Areas

To test the simulator functionalities under extreme conditions, we consider in this case study that the initiating event is the sudden split of the northern and southern areas of the Nordic system. Specifically, all tie-lines (i.e., 27-30, 30-15, 29-34, 34-15, 29-35, 35-36, 31-33, 33-14, 31-32, and 32-14) are

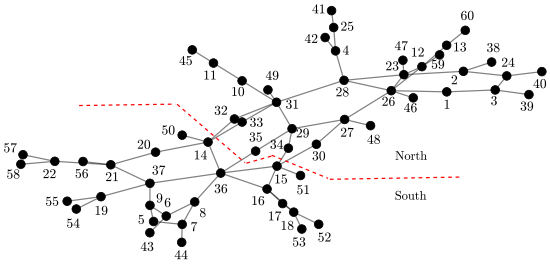

Figure 3. Topology of Nordic power system before contingency.

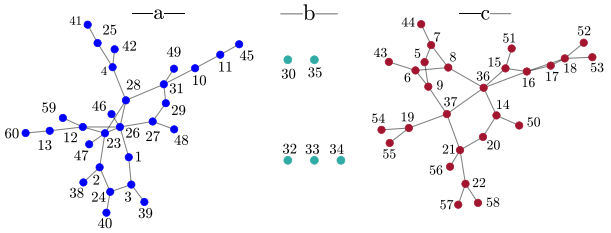

Figure 4. Detected islands by the proposed LIBID algorithm including a) island 1, b) isolated buses, and c) island 2.

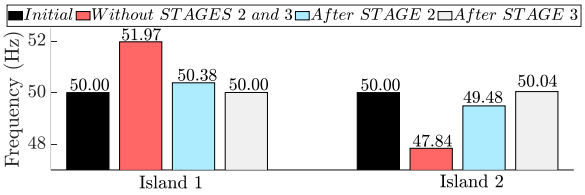

Figure 5. Frequency of islands 1 and 2 in different stages.

disconnected simultaneously e.g., as a result of network splitting protection malfunction. Note that this particular case examines a single cascade (i.e. a single one-time execution of *STAGES 1* to *3*) because after the execution of *STAGES 1* to *3*, no further violations of the line flow limits occur, ending the cascades.

1) Performance of the Proposed Method in Islanding Detection

Fig. 3 shows the network topology before the contingency. This topology is generated by the proposed LIBID algorithm, demonstrating that is works correctly in the specific case where there is only one island, i.e. entire network is connected.

Fig. 4 shows the detected islands immediately after the split of the northern and southern areas as a result of *STAGE* 1. Observe that the proposed LIBID algorithm detects accurately the resulting islands, i.e., island 1 (north), island 2 (south), and the isolated buses. The latter case is also used to verify that the algorithm detects the islands containing one bus.

2) Performance of the Proposed Method in Analysis of System Frequency

Fig. 5 shows the frequency of each island before the initiating event and after it, without any control action (without *STAGES 2* and *3*), and after the implementation of *STAGES 2* and *3*. It can be observed that, both islands have initially the same frequency, i.e., 50.00 Hz. After the event, when there are no control actions in the system, the frequency of island 1 and island 2 is 51.97 Hz

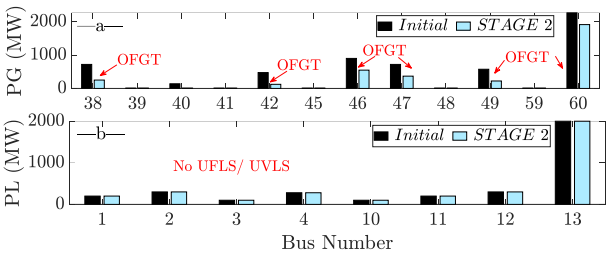

Figure 6. Active power generation and load demand in island 1.

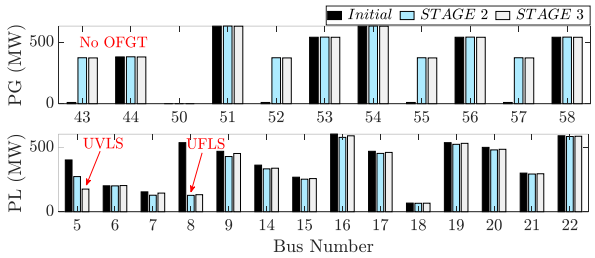

Figure 7. Active power generation and load demand in island 2.

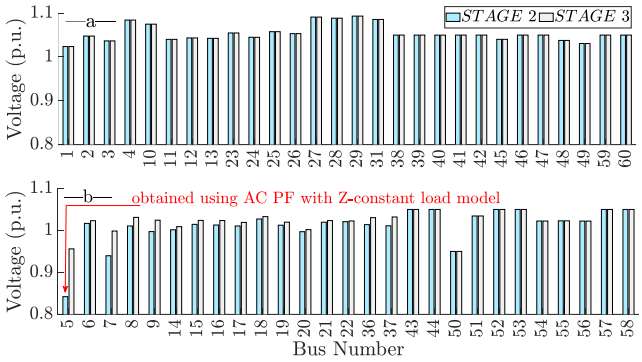

Figure 8. Voltage of different buses of a) island 1 b) island 2.

and 47.84 Hz, respectively. This means that islands 1 and 2 experience over-frequency and under-frequency, respectively. Therefore, as Fig. 6 (a) shows, for island 1, there are some automatic OFGT in *STAGE 2*, and as Fig. 6 (b) shows, there is no need for UFLS. Conversely, according to Fig. 7, there is no need for OFGT in island 2, and UFLS is performed at bus 8 (as the highest priority bus in island 2). It can be seen in Fig. 5 that these OFGT and UFLS result in restoring the frequency to allowable values, e.g., 50.38 Hz and 49.49 Hz in islands 1 and 2, respectively.

Note that such frequency adjustment is performed considering the change in generator power due to PFC and also the maximum/minimum active power limit of each generator.

3) Performance of the Proposed Method in Analysis of System Voltage

After the frequency adjustment, the proposed method proceeds by checking the voltage of the different islands. Fig. 8 indicates that the voltage of all the buses on island 1 is by chance within the allowable range after *STAGE 2*. Therefore, as Fig. 6 shows, island 1 does not need UVLS, so the voltage of all buses

TABLE II. CASE STUDY 2: RESULTS OF CASCADING OUTAGE SIMULATION

Cascade 1	*STAGE 1:* 1 island detected (i_1 including whole network)			
	STAGE 2:	i_1		
	Frequency with no action (Hz)	50.09		
	OFGT or UFLS	No		
	Frequency after OFGT or UFLS	-		
	AC PF constant PQ or Z	PQ		
	STAGE 3:	i_1		
	Voltage limit violation	No		
	UVLS	-		
Line flow limit violation is detected. Line 23-28 is disconnected				
Cascade 2	*STAGE 1:* 1 island detected (i_1 including whole network)			
	STAGE 2:	i_1		
	Frequency with no action (Hz)	50.09		
	OFGT or UFLS	No		
	Frequency after OFGT or UFLS	-		
	AC PF constant PQ or Z	PQ		
	STAGE 3:	i_1		
	Voltage limit violation	No		
	UVLS	-		
Line flow limit violation is detected. Lines 26-27, 26-28, and double circuit lines 1-3, 2-24, and 3-24 are disconnected				
Cascade 3	*STAGE 1:* 4 islands detected: i_1 ={1, 2, 12, 13, 23, 26, 38, 46, 47, 59, 60}, i_2 ={4, 5, 6, 7, 8, 9, 10, 11, 14, 15, 16, 17, 18, 19, 20, 21, 22, 25, 27, 28, 29, 30, 31, 32, 33, 34, 35, 36, 37, 41, 42, 43, 44, 45, 48, 49, 50, 51, 52, 53, 54, 55, 56, 57, 58}, i_3 ={3, 39}, and i_4 ={24, 40} without any load.			
	STAGE 2:	i_1	i_2	i_3
	Frequency with no action (Hz)	53.67	48.94	49.15
	OFGT or UFLS	OFGT	UFLS	UFLS
	Frequency after OFGT or UFLS	50.14	49.54	49.75
	AC PF constant PQ or Z	PQ	PQ	PQ
	STAGE 3:	i_1	i_2	i_3
	Voltage limit violation	No	No	No
	UVLS	-	-	-
No more line flow limit violation is detected				

Cascading metrics	***LO***	***LNS (MW)***	***GT (MW)***
	10	318.2	465.9

Loads shed by UFLS: Buses 1 and 5.
Loads shed by UVLS: No

in *STAGES 2* and *3* is the same, as shown in Fig. 8 (a). However, in island 2, the voltage of bus 5 is 0.84 p.u., which is below the minimal limit. Therefore, as shown in Fig. 7, UVLS is performed in bus 5 of island 2. Fig. 8 shows that performing such UVLS in *STAGE 3* leads to an improvement in the voltage profile of island 2. In particular, the voltage of bus 5 increases to 0.96 p.u., which is within the acceptable range.

It should be noted that the low voltage condition on island 2 at *STAGE 2* leads to divergence of conventional AC PF and stops the simulation of the cascaded outage. As explained earlier, existing methods cannot capture such cases and the proposer operation of UVLS by the methods based on DC PF [5]-[8] and cannot be accurately implemented by some other methods [9]-[20] that handle this problem using uniform load shedding that is not complied with what exists in real-world. On the other hand, as shown in Fig. 8 (b), the voltage profile of island 2 at *STAGE 2* is calculated thanks to the advantage of the extended AC PF to transform the PQ-constant load model into a Z-constant model. Subsequently, the UVLS in *STAGE 3* is performed using such an AC PF model, resulting in estimation of voltage profile and successful simulation of cascading outages.

B. Case Study 2: Initial Event: Outage of Line 23-26

Table II shows the results of the simulation of cascading outage triggered by the outage of line 23-26. It can be observed that this initiating event results in three cascades. In the first

cascade (immediately after the outage of line 23-26), the proposed LIBID islanding detection algorithm detects only one island in the whole network, which means that this triggering event does not lead to any islanding in the network. Moreover, this single contingency does not lead to any frequency or voltage violation in the system. Therefore, as indicated in Table II, there is no need for OFGT/UFLS and UVLS in the first cascade. However, the initiating event under study results in the flow limit of line 23-28 being exceeded.

In cascade 2, the additional outage of line 23-28 does not result in the formation of a new island or violate the voltage or frequency in the system. However, the combination of these two outages results in a violation of the flow limits for an additional 8 transmission lines, as indicated in Table II. Therefore, by disconnected these 8 lines, the network in cascade 3 is split into 4 islands i_1, i_2, i_3, and i_4 as described in Table II. Island 4 contains no load demand, so it loses the generator. In the three other islands, over-frequency, under-frequency, and over-frequency are observed, respectively. By simulating OFGT or UFLS in these three islands, a frequency of 50.14, 49.54, and 49.75 Hz is recovered, which is within the allowable range. After that, the *STAGE 3* identifies no voltage violation on any of the islands. Finally, since there is no more line flow violation, the cascade simulation terminates. It should be noted due to these good voltage conditions AC PF with PQ-constant load model converges, and it is not necessary to use AC PF with Z-constant load model.

Cascading metrics are provided in Table II, showing that a total of 10 lines are disconnected, 318 MW (3.65%) of system load is not supplied, and about 466 MW of generation is tripped.

As regards computation time, it is worth noting that for the extensive simulations like those presented so far, the proposed simulator executes fast in under 0.02 seconds.

IV. Conclusions and Future Works

The paper has proposed a new comprehensive framework for the simulation of cascading failures, considering the main needed modelling features i.e., the detection of islanding and handling frequency and voltage issues. Simulation results have shown that:

- the proposed LIBID algorithm accurately detects the islands that may occur after the initiating or subsequent events;
- the frequency change of each island during cascading outages is accurately simulated considering the effects of PFC, possible UFLS/OFGT, grid effects and active power limits of generators thanks to the proposed extended AC PF;
- by using an enhanced modeling of UVLS and load, any divergence of AC PF is avoided, and the proposed cascading outage simulator can proceed even in voltage unstable cases where UVLS is triggered and counteract voltage instability.

The simulator calculates three metrics: the number of line outages, the amounts of load not supplied, and generation tripped.

The proposed extended AC PF-based cascading simulator is not only comprehensive and accurate but also efficient, since its simulation time is in order of 10^{-2} seconds for a 60-bus system. This short time suggests the simulator scales to large systems. Indeed, no scalability issues are to be expected since the method relies on a sequence of enhanced AC power flow calculations.

Our future work will consider the following items.

- Here, all overloaded lines are simultaneously disconnected. However, after the first line outage, the power flows will change, so different lines might be overloaded. Hence, a probabilistic model can be used to determine what happens depending on which line trips first.
- The method can be further extended to incorporate switchable shunt reactors / capacitors, as well as accounting for uncertainty in the response of the system protection scheme (e.g., the possibility of malfunction).

Acknowledgment

The authors acknowledge the funding from Luxembourg National Research Fund (FNR) in the framework of the project TESTIFY (C21/SR/15762760).

References

[1] M.Z. Zakariya, J. Teh, "A Systematic Review on Cascading Failures Models in Renewable Power Systems with Dynamics Perspective and Protections Modeling," Electric Power Systems Research, vol. 214, pp. 108928, 2023.

[2] Vaiman et al., "Risk Assessment of Cascading Outages: Methodologies and Challenges," IEEE Transactions on Power Systems, vol. 27, no. 2, pp. 631-641, 2012.

[3] T. Guler, and G. Gross, "Detection of Island Formation and Identification of Causal Factors Under Multiple Line Outages," IEEE Transactions on Power Systems, vol. 22, no. 2, pp. 505-513, 2007.

[4] F. Goderya, A. A. Metwally, and O. Mansour, "Fast Detection and Identification of Islands in Power Networks," IEEE Transactions on Power Apparatus and Systems, vol. PAS-99, no. 1, pp. 217-221, 1980.

[5] M. J. Eppstein and P. D. Hines, "A "random chemistry" algorithm for identifying collections of multiple contingencies that initiate cascading failure," IEEE Transactions on Power Systems, vol. 27, no. 3, pp. 1698-1705, 2012.

[6] Dobson, B. A. Carreras, V. E. Lynch, and D. E. Newman, "An initial model for complex dynamics in electric power system blackouts," in hicss, 2001.

[7] Liu, X. Zhang, and K. T. Chi, "Effects of high level of penetration of renewable energy sources on cascading failure of modern power systems," IEEE Journal on Emerging and Selected Topics in Circuits and Systems, vol. 12, no. 1, pp. 98-106, 2022.

[8] M. A. Rios, D. S. Kirschen, D. Jayaweera, D. P. Nedic, and R. N. Allan, "Value of security: modeling time-dependent phenomena and weather conditions," IEEE Transactions on Power Systems, vol. 17, no. 3, pp. 543-548, 2002.

[9] D. S. Kirschen, D. Jayaweera, D. P. Nedic, and R. N. Allan, "A probabilistic indicator of system stress," IEEE Transactions on Power Systems, vol. 19, no. 3, pp. 1650-1657, 2004.

[10] D. P. Nedic, I. Dobson, D. S. Kirschen, B. A. Carreras, and V. E. Lynch, "Criticality in a cascading failure blackout model," International Journal of Electrical Power & Energy Systems, vol. 28, no. 9, pp. 627-633, 2006.

[11] M. Rios, K. Bell, D. Kirschen, and R. Allan, "Computation of the value of security," Manchester Centre for Electrical Energy, UMIST, EPSRC/ERCOS reference nGR/K, vol. 80310, 1999.

[12] B. Gjorgiev and G. Sansavini, "Nexus-e: Cascades Module Documentation," ETH Zurich, 2020.

[13] S.-W. Mei, X.-F. Weng, and A.-C. Xue, "Blackout model based on OPF and its self-organized criticality," in 2006 Chinese control conference, 2006: IEEE, pp. 1673-1678.

[14] S. Mei, Y. Ni, G. Wang, and S. Wu, "A study of self-organized criticality of power system under cascading failures based on AC-OPF with voltage stability margin," IEEE Transactions on Power Systems, vol. 23, no. 4, pp. 1719-1726, 2008.

[15] P. Henneaux, P.-E. Labeau, J.-C. Maun, and L. Haarla, "A two-level probabilistic risk assessment of cascading outages," IEEE transactions on power systems, vol. 31, no. 3, pp. 2393-2403, 2015.

[16] I. Dobson, "Estimating the propagation and extent of cascading line outages from utility data with a branching process," IEEE Transactions on Power Systems, vol. 27, no. 4, pp. 2146-2155, 2012.
[17] P. D. Hines, I. Dobson, and P. Rezaei, "Cascading power outages propagate locally in an influence graph that is not the actual grid topology," IEEE Transactions on Power Systems, vol. 32, no. 2, pp. 958-967, 2016.
[18] S. Gharebaghi, S. G. Vennelaganti, N. R. Chaudhuri, T. He, and T. F. La Porta, "Inclusion of pre-existing undervoltage load shedding schemes in AC-QSS cascading failure models," IEEE Transactions on Power Systems, vol. 36, no. 6, pp. 5645-5656, 2021.
[19] M. Noebels, R. Preece, and M. Panteli, "AC cascading failure model for resilience analysis in power networks," IEEE Systems Journal, vol. 16, no. 1, pp. 374-385, 2020.
[20] R. Yao, S. Huang, K. Sun, F. Liu, X. Zhang, and S. Mei, "A multi-timescale quasi-dynamic model for simulation of cascading outages," IEEE Transactions on Power Systems, vol. 31, no. 4, pp. 3189-3201, 2015.
[21] S. Gharebaghi, N. R. Chaudhuri, T. He, and T. La Porta, "An approach for fast cascading failure simulation in dynamic models of power systems," Applied Energy, vol. 332, p. 120534, 2023.
[22] J. Song, E. Cotilla-Sanchez, G. Ghanavati and P. D. H. Hines, “Dynamic modeling of cascading failure in power systems,” IEEE Transactions on Power Systems, vol. 31, no. 3, pp. 2085-2095, May 2016.
[23] X. Gao, M. Peng, C. K. Tse and H. Zhang, "A Stochastic Model of Cascading Failure Dynamics in Cyber-Physical Power Systems," in IEEE Systems Journal, vol. 14, no. 3, pp. 4626-4637, 2020.
[24] A. J. Flueck, I. Dobson, Z. Huang, N. E. Wu, R. Yao, and G. Zweigle, “Dynamics and Protection in Cascading Outages,” 2020 IEEE Power & Energy Society General Meeting (PESGM), Montreal, QC, 2020, pp. 1-5.
[25] A. Zobian and M. Ilic, "Unbundling of transmission and ancillary services, part 1: Technical issues, and part 2: Cost-based pricing framework," IEEE Power Engineering Review, vol. 17, no. 5, pp. 52-52, 1997.
[26] L. Mirsky, An introduction to linear algebra. Courier Corporation, 2012.
[27] F. Capitanescu, "Suppressing ineffective control actions in optimal power flow problems," IET Generation, Transmission & Distribution, vol. 14, no. 13, pp. 2520-2527, 2020.